catalysts

MDPI

Article

Preparation of High-Performance Zn-Based Catalysts Using Printing and Dyeing Wastewater and Petroleum Coke as a Carrier in Acetylene Acetoxylation

Yuhao Chen [1], Mengli Li [1], Zhuang Xu [1], Guowang Shen [1], Xugeng Wang [1,2,*] and Bin Dai [1,2,*]

[1] School of Chemistry and Chemical Engineering, Shihezi University, Shihezi 832000, China
[2] Key Laboratory for Green Processing of Chemical, Engineering of Xinjiang Bingtuan, Shihezi 832000, China
* Correspondence: wxgen@shzu.edu.cn (X.W.); db_tea@shzu.edu.cn (B.D.);
Tel.: +86-993-2057270 (B.D.); Fax: +86-993-2057210 (B.D.)

Abstract: In this study, novel Zn catalysts were prepared by the wet impregnation method using printing and dyeing wastewater (PDW)-modified petroleum coke (petcoke) as a carrier, and they were applied to the acetylene acetoxylation. The pretreated petroleum coke has a high specific surface area which provides sufficient space for the loading of Zn. Calcination further increases catalyst activity, but when calcination temperatures exceed 1000 °C, a significant loss of Zn occurs, resulting in a dramatic decrease in catalyst activity. This enables the conversion of acetic acid up to 85%. X-ray photoelectron spectroscopy confirmed that a large amount of N is introduced into PC from PDW, which changes the electron transfer around Zn. Temperature-programmed desorption (TPD) analysis revealed that the nitrogen-doped $Zn(OAc)_2$ catalyst enhanced the catalytic activity by modulating the intensity of the catalyzed adsorption of acetic acid and acetylene. This study provides a new way to reuse petroleum coke and printing and dyeing wastewater to support the sustainable development of the vinyl acetate industry.

Keywords: wastewater; petroleum coke; vinyl acetate

check for updates

Citation: Chen, Y.; Li, M.; Xu, Z.; Shen, G.; Wang, X.; Dai, B. Preparation of High-Performance Zn-Based Catalysts Using Printing and Dyeing Wastewater and Petroleum Coke as a Carrier in Acetylene Acetoxylation. *Catalysts* **2023**, *13*, 539. https://doi.org/10.3390/catal13030539

Academic Editor: Carlo Santoro

Received: 18 January 2023
Revised: 15 February 2023
Accepted: 24 February 2023
Published: 8 March 2023

1. Introduction

Along with the rapid development of the chemical industry, environmental problems have become increasingly prominent, and the concept of green chemistry has been emphasized. Global production of petroleum coke (petcoke) has reached 150 million metric tons per year and is expected to increase in the future due to the gradual increase in the heaviness of crude oil [1], which is a solid-rich carbon produced during the upgrading of heavy oil in refineries and delayed vacuum slag coking [2]. Given the limitations of conventional gasification and combustion processes in terms of efficiency and environmental friendliness [3,4], scientists should search for an alternative technology for handling large quantities of petcoke. Printing and dyeing wastewater (PDW) is the wastewater discharged from printing and dyeing, wool dyeing and finishing, and silk factories, which mainly process cotton, hemp, chemical fibers, their blended products, and silk. Printing and dyeing plants produce large volumes of wastewater, and each printing and dyeing process consumes about 200 t of water per 1 ton of textiles, of which 80–90% becomes wastewater discharge. PDW is characterized by a large volume of water, high content of organic pollutants, high alkalinity, and large changes in water quality and it contains heavy metal elements; it is one of the more difficult industrial wastewaters to be treated [5,6]. The current treatment method covers a large area, with considerable investment and high treatment cost. The value-added application of PDW cannot only transform waste into valuable materials but also solve environmental problems. Therefore, studies should focus on the novel uses of PDW [5–8].

Many studies have been conducted on the use of petcoke as a catalyst carrier. Jinsoon Choi et al. [9] achieved a high activity by activating and converting petcoke into catalyst carriers and prepared nickel catalysts for toluene hydrogenation by wet impregnation. After the activation of petcoke with KOH, Liu et al. [10] prepared mesoporous materials with high specific surface area for use as carriers for esterification reactions with very good properties. J. A. Arcibar-Orozco et al. [11] used petcoke as a ZnO-based photocatalyst carrier, which acted as a carbon additive to improve the semiconductor photocatalytic performance. These findings showed that petcoke has great potential as a catalyst carrier. In addition, Shuang Mei et al. [12] used the abundant N in PDW to modify the carrier and applied it to acetylene salt acidification, which can effectively improve the catalyst activity. A new method of PDW treatment involves the modification of the catalyst carrier. Therefore, we intended to synthesize a new catalyst carrier using petcoke and PDW.

The price of vinyl acetate has been rising in recent years and demand is increasing. For the production of vinyl acetate, there are currently two main methods used in industry to produce vinyl acetate: the acetylene method and the ethylene method, with the acetylene method still occupying the larger part of applications, especially in coal-rich regions. The catalyst for the preparation of vinyl acetate by the acetylene method, currently almost always used in industry, is zinc acetate loaded on activated carbon (Zn/AC), but this catalyst has low activity and poor stability, requiring frequent replacement of the catalyst, leading to increased costs. Based on previous studies, Wang [13] found that an increase in nitrogen enhanced the activity of acetylene acetylation. Hou [14] et al. also prepared a nitrogen-containing catalyst with high catalytic activity, and Xu [15] et al. also prepared a highly active Zn/NC catalyst using an in situ generation method, indicating that N has a large effect on the reaction, and PDW contains a large amount of N. In contrast, catalysts prepared using PC and PCW are not only more active, but also reduce production costs to some extent, while also achieving waste utilization.

In this paper, we studied the use of KOH to expand the pores of petcoke. The active alkaline ions penetrated into the petcoke microcrystals to act as a skeleton in pore formation and provide a sufficiently large specific surface area. Petcoke can be used to adsorb PDW after pore expansion, and substances in PDW can be used to modify the petcoke to change the surface chemical environment. After treatment, a petcoke-based carrier was obtained, and we applied this carrier to prepare vinyl acetate by the acetylene and acetic acid method and achieved a high activity. The high activity was characterized by the Brunauer–Emmett–Teller (BET) method, inductively coupled plasma mass spectrometry (ICP-MS), X-ray photoelectron spectroscopy (XPS), Fourier transform infrared (FTIR), and temperature-programmed desorption (TPD).

2. Results and Discussion

2.1. Activity Test

Due to the unstable flow rate at the beginning of the reaction and the uneven mixing of acetylene gas and acetic acid vapor, the activity of the catalyst was low for the first two hours and stabilized after two hours. The activity of different catalysts was tested at the reaction temperature of 220 °C, C_2H_2 gas at an hourly space velocity of 500 h^{-1}, and a C_2H_2 to acetate acid ratio of 3:1. Figure 1a shows the activity of catalysts calcined at different temperatures. At the calcination temperatures of 500 °C–600 °C, the catalyst activity hardly changed. However, when the calcination temperature reached 800 °C, the catalyst activity increased to a certain extent, and the greatest increase occurred at 900 °C, at which the activity increased to more than 80%. The increase in activity continued until the calcination temperature of 1000 °C, at which point the catalyst activity decreased sharply. Calcination increased the specific surface area and void volume of the carrier and burned off certain impurities, which exposed more active sites, redispersed active components, and increased contact opportunities with raw materials, thus improving reactivity. After the calcination at 1000 °C, the activity dropped to almost zero, and we assumed that the active component

zinc was lost at this point. The ICP-MS data showed that after the calcination at 1000 °C, the zinc in the catalyst was almost gone, and, thus, the catalyst lost its activity.

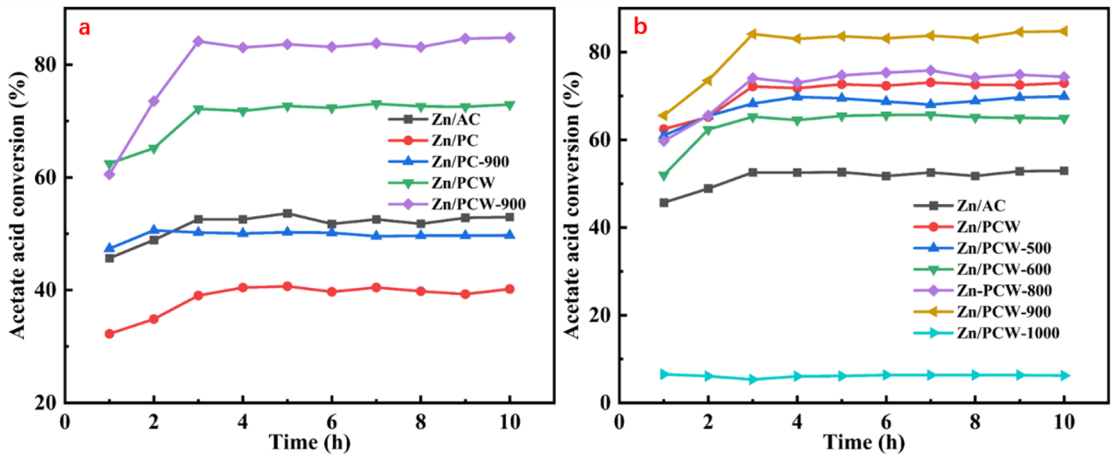

Figure 1. Conversion of acetic acid of Vinyl acetate with Zn/PC, Zn/AC, Zn/PCW, and Zn/PCW-900 (**a**) and conversion of acetic acid with Zn/PCW at different calcination temperatures (**b**).

Figure 1b displays the activity comparison of Zn/AC, Zn/PC-900, Zn/PC, Zn/PCW, and Zn/PCW-900. Zn/PC (catalyst prepared with petcoke but not treated with PDW as a carrier) had the lowest activity, and the acetic acid conversion was approximately 40%. After modification with PDW, the activity of Zn/PCW increased substantially, and the acetic acid conversion rate reached more than 70%. Compared with the common Zn/AC, the activity increased by about 0.4 times. After calcination at the screened optimal calcination temperature of 900 °C, the activity further increased and reached up to 85%. Meanwhile, we also calcined Zn/PC at 900 °C and obtained Zn/PC-900, whose catalytic activity was almost unchanged.

2.2. Catalyst Characterization

2.2.1. N_2 Physical Adsorption and Desorption

The structural changes of petcoke before and after modification and the differences in the modified petcoke compared with ordinary AC were investigated by low-temperature nitrogen physical adsorption. Table 1 lists the specific surface area, total pore volume, and average pore size of the modified petcoke and AC under different conditions. The BET specific surface area of the PCW carrier obtained from petcoke after pore expansion modification treatment can reach 1505.3 m^2/g. The larger specific surface area, pore volume, and pore size were conducive to the adsorption of active components and could provide more active sites. Zn/AC and Zn/PCW were obtained by direct drying of equal proportions of Zn acetate loaded on AC and PCW using the excess impregnation method. This finding indicates that zinc acetate entered the pore channels of PCW and occupied the space inside, which resulted in a large reduction in BET specific surface area and pore volume while not blocking the pore pathway and not changing the average pore size, allowing the reaction mass transfer to proceed smoothly. Figure 2a shows the N_2 physical isotherm adsorption lines. PCW exhibited type I isotherms, with a phase of rapidly increasing adsorption at low relative pressures of 0 p/p_0 to 0.1 p/p_0, which is typical of the microporous filling of microporous adsorbent species. This result indicates the presence of a large number of microporous pores in the PCW species [16]. At 0.4–0.7 p/p_0, an evident H4-type hysteresis loop was observed, and it was due to the capillary coalescence that caused the nitrogen molecules to condense to fill the mesoporous pore channels at lower than atmospheric pressure. The beginning of capillary coalescence occurred at the liquid surface of the annular adsorption film of the pore wall, and desorption started from the liquid surface of the spherical bent moon of the pore, which indicated the presence of mesopores in PCW. AC exhibited a type IV isothermal curve. The same H4-type hysteresis loop was present, which

is a typical curve for microporous–mesoporous materials [17]. Figure 2b shows the pore size distribution. The pore size of Zn/AC was mainly distributed in the range of 2–5 nm, which is mainly mesoporous. By contrast, Zn/PCW was more microporous. According to studies [18,19], the increased number of micropores is favorable for the reaction.

Table 1. Physical-chemical properties of the different catalysts.

Sample	AC	Zn/AC	PCW	Zn/PCW	Zn/PCW-600	Zn/PCW-900	Zn/PCW-1000
S_{BET} (m^2/g)	1476.9	629.9	1505.3	86.3	1105.8	1126.8	1412.3
Pore volume (cm^3/g)	0.67	0.28	0.80	0.05	0.50	0.51	0.63
Average pore diameter (nm)	1.81	1.8	2.1	2.3	1.80	1.81	1.79

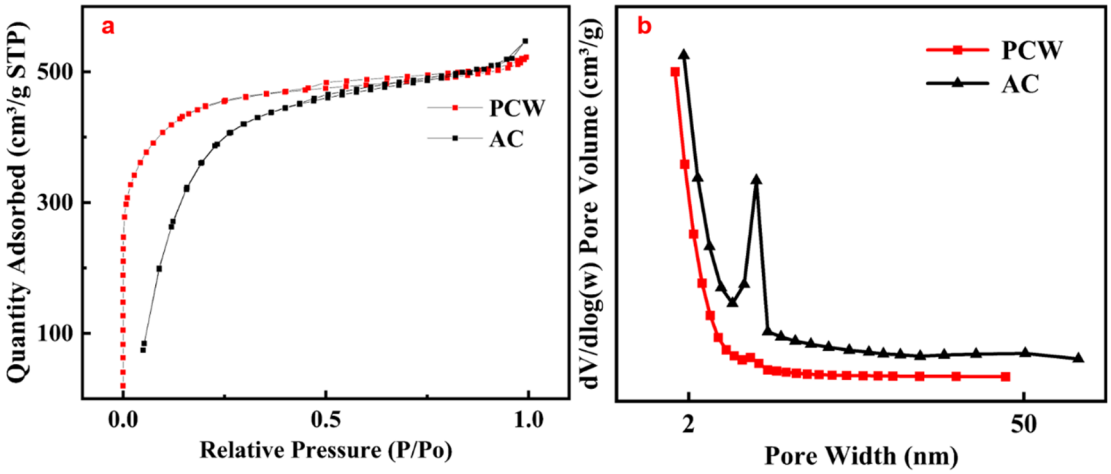

Figure 2. (**a**) Nitrogen (N_2) adsorption and desorption isotherms and (**b**) pore size distributions of AC and PCW.

After further calcination of the produced Zn/PCW, the BET surface area of the catalyst increased to about 1100 m^2/g and the pore volume increased to about 0.5 cm^3/g. This is because the high temperature caused the decomposition of the larger molecular weight of Zn acetate into smaller ZnO particles and some impurities were burned off during the calcination process, which increased the BET surface area and pore volume.

The specific surface area and pore volume increase, which exposes more active sites. However, after calcination at 1000 °C, the BET surface area was almost the same as that of PCW, which may due to the fact that most of the zinc has been lost at that temperature.

2.2.2. ICP-MS

The Zn content of the active component in different catalysts was tested using ICP-MS, where the Zn contents of Zn/AC, Zn/PCW, and Zn/PC were 14.01%, 13.75%, and 12.21%, respectively, showing almost no difference. Combined with the data in Table 2, the Zn contents on the surface of Zn/AC and Zn/PC catalysts measured by XPS were 12.54% and 12.11%, respectively, and that of Zn/PCW was 6.05%, which indicated that most of the Zn was not deposited on the catalyst surface for Zn/AC and Zn/PC but entered the catalyst interior and dispersed in the catalyst pores. These results were consistent with those of N_2 physical adsorption and desorption. After the calcination at 900 °C, the Zn content was 11.98% with minimal loss, but that in the catalyst was almost absent at the calcination temperature of 1000 °C, which indicated that most of the Zn acetate had been lost at this temperature. The Zn content in the catalyst was reduced to 0.52% after the calcination at 1000 °C, which was consistent with the BET data. The BET surface area of Zn/PCW-1000 was almost the same as that of PCW (Table 3).

Table 2. Zn content on XPS (wt%).

Sample	Zn/AC	Zn/PCW	Zn/PC
Zn	12.54	6.15	12.11
N	3.36	7.84	1.75

Table 3. Zn content on ICP (wt%).

Sample	Zn/AC	Zn/PCW	Zn/PCW-900	Zn/PCW-1000	Zn/PC
Zn (wt%)	14.01	13.75	11.98	0.52	12.21

2.2.3. XPS (X-ray Photoelectron Spectroscopy)

To investigate the elemental changes in the catalyst and to evaluate in more detail the effect between N and Zn, XPS tests were carried out on Zn/PC as well as Zn/PCW. The survey spectrum of Zn/PC and Zn/PCW is shown in Figure 3. Here, there are some differences in C1s, O1s, N1s, and Zn2p. The spectral peaks of Zn/PCW are both higher than those of Zn/PC. Especially for N1s, there are almost no spectral peaks in Zn/PC. This indicates that the PDW introduced N elements to the petcoke and also affected other chemical environments such as C1s and O1s on the petcoke surface. The elemental content of N by XPS also shows that Zn/PCW contains 7.84% N, while Zn/PC contains only 1.75% N and also more compared with Zn/AC at 3.36%.

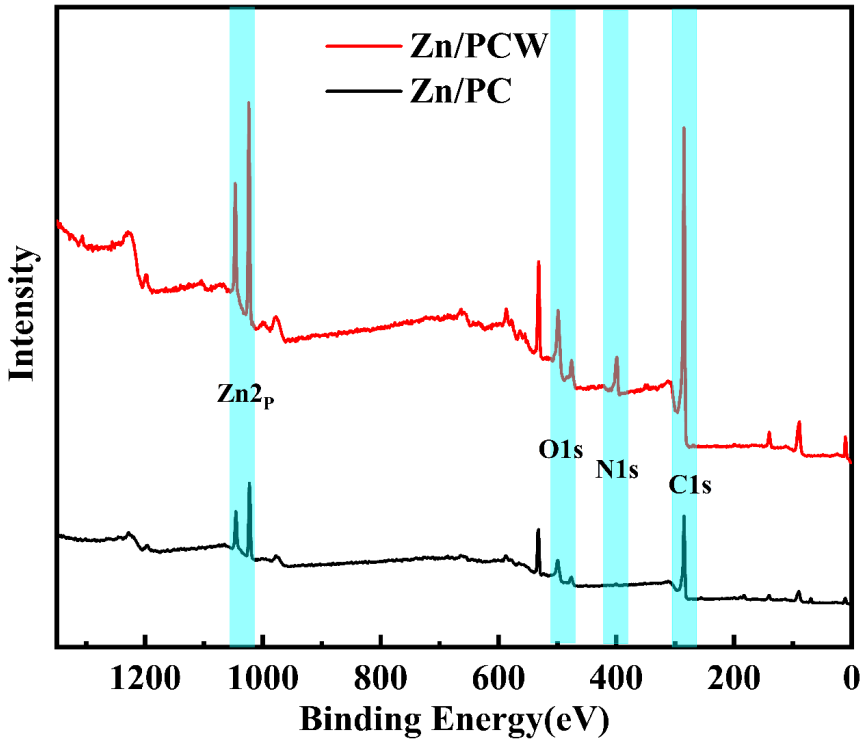

Figure 3. XPS survey spectrum of Zn/PC and Zn/PCW.

As presented in Figure 4a, the Zn2p orbitals in Zn/PCW shifted compared with those in Zn/AC. This result implied that after the introduction of petcoke and AC into the wastewater, the PDW affected the properties of the carrier surface, and some PDW substances were adsorbed on the petcoke during treatment. The peak positions of Zn2p shifted to a lower field, and the electron cloud density around Zn was reduced, which favored the adsorption of acetic acid. After calcination, a portion of Zn2p was still bound to petcoke and coordinated with Zn acetate during loading, which changed the electron cloud density

around Zn. The N1s XPS spectrum of Zn/PCW (Figure 4d) showed peaks at 400.7, 398.9, and 398.2 eV, which represented pyrrole-N, Zn-N, and pyridine-N, respectively [20–22]. Zn/PC had a very low peak at 401.4 eV, which indicated that it contained a small amount of nitrogen [23]. Pyridine-N and pyrrole-N were mainly introduced on the surface of petcoke in PDW, and the peak at 398.9 eV in Zn/PCW revealed the presence of a Zn-N bond, which meant that the introduced N was coordinated with the active component Zn [14,23]. The O1s pattern in Figure 4b shows the binding energy of Zn/PC and Zn/PCW. O1s can be fitted into three peaks at 531.8, 532.6, and 533.5 eV in Zn/PCW, which represent Zn–OH, C–O, and C=O [24,25], respectively; meanwhile, the peak positions in Zn/PC were 531.8, 532.7, and 533.7 eV. The latter two peaks shifted, which indicated that the chemical environment around the O on the petcoke surface also changed. The C1s spectrum in Figure 4c comprised peaks at 284.8, 285.8, and 289.2 eV, which corresponded to C=C, C–C, and O–C=O bonding, respectively; meanwhile, the peak positions in Zn/PC were observed at 284.7, 285.8, and 288.9 eV [26,27]. As with O1s, this finding suggests that the chemical environment around the petcoke surface C also changed with the introduction of PDW. However, the change in C and O on the surface of petcoke was negligible, and the most considerable change was that of N. Therefore, the doping of N was the main role of modified petcoke in PDW.

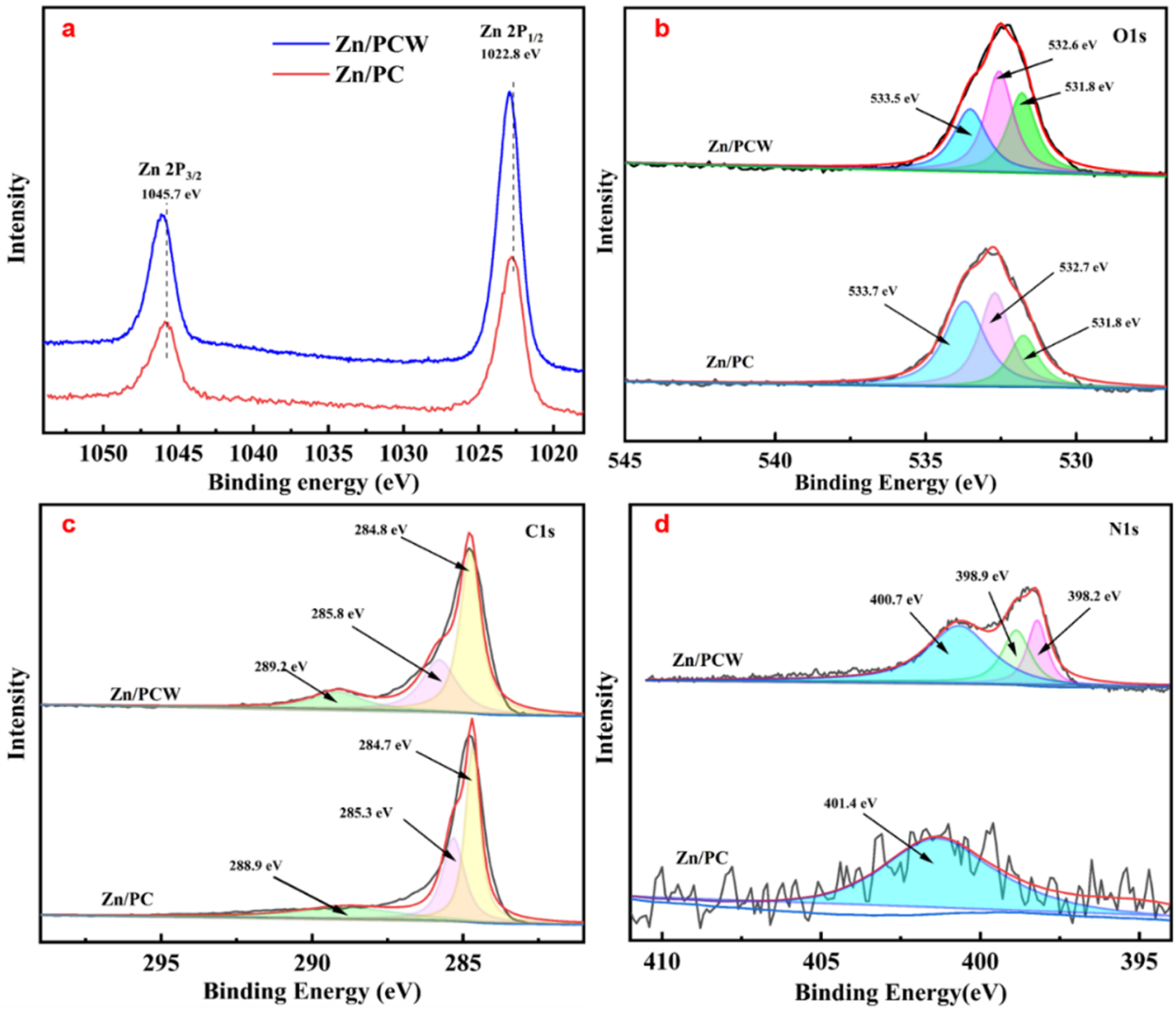

Figure 4. XPS spectra of Zn 2p of Zn/PC and Zn/PCW (**a**) and (**b**) N1s,(**c**) C 1s, and (**d**) O1s of PCW.

2.2.4. FTIR (Fourier Transform Infrared Spectrometer)

In order to evaluate the changes in functional groups on the catalyst in more detail, FTIR analysis was carried out on PC and PCW. Figure 5 shows the FTIR spectrum of the PC and PCW. Compared with those of PC, the FTIR spectra of PCW showed distinct peaks at 3440, 2900, 2370, 1640, and 1420 cm^{-1}. The medium intensity peak at 3400 cm^{-1} was the stretching vibration of NH in primary amines [28]. The absorption peaks at approximately 2930 and 2860 cm^{-1} can be related to aldehyde–CH stretching vibrations, and the band at 2370 cm^{-1} can prove the presence of N=C=O [29]. The absorption peaks at 1640 and 1440 cm^{-1} were C=O and H–C–H stretching vibrations (deformations) [29], respectively. The wastewater introduced some nitrogenous oxygen-containing groups on the PC surface, which may be one of the reasons for the elevated activity.

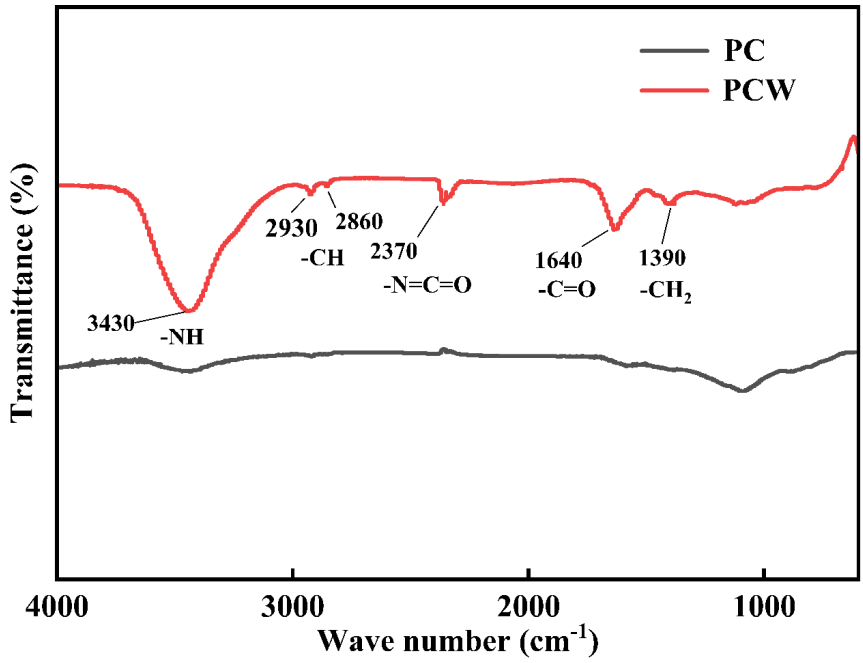

Figure 5. TIR spectra of PC and PCW.

2.2.5. TPD (Temperature-Programmed Desorption)

TPD tests were performed on Zn/PCW and Zn/AC to observe the adsorption characteristics of catalysts on the reactants, and the results are shown in Figure 6. The area of the desorption peak indicates the adsorption capacity of the reactants, and the desorption temperature denotes their adsorption intensity [30]. Compared with Zn/AC, the desorption temperature of acetylene by Zn/PCW increased from 329 °C to 392 °C. Although the desorption temperature increased, the amount of acetylene adsorbed decreased significantly. For the adsorption of acetic acid, the desorption temperature of Zn/PCW increased from 347 °C to 374 °C compared with that of Zn/AC, and the adsorption of acetic acid also increased significantly. These results indicate that Zn/PCW had a weaker adsorption capacity for acetylene but a greater adsorption capacity for acetic acid [15,25]. This finding may be due to some organic molecules and metal ions in the wastewater that were adsorbed on the catalyst surface, and they ligated with Zn during impregnation. As a result, the electron cloud density of Zn changed, which strengthened the Zn adsorption capacity for acetic acid and reduced the adsorption capacity for acetylene. This finding was consistent with the weakened electron cloud of Zn density and the shift of the binding energy toward the high field in XPS.

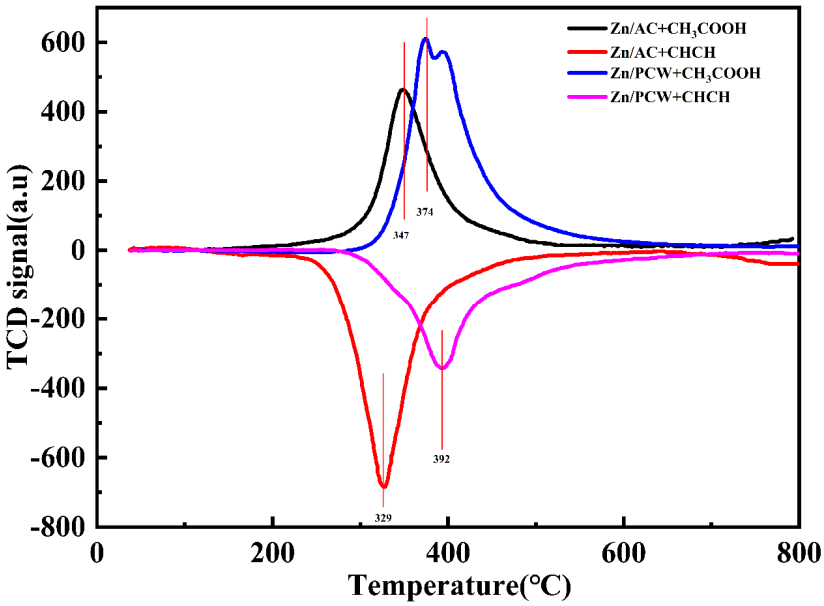

Figure 6. TPD results of Zn/AC and Zn/PCW with CH_3COOH and C_2H_2. TCD = Thermal conductivity detector.

3. Experiment

3.1. Raw Materials

The PDW in this study was obtained from Ruyi Textile Factory in Shihezi, Xinjiang, China, which is a textile factory group that conducts cotton fabric dyeing. The petcoke (Urumqi Petrochemical Company) contained carbon (90–97%) as the main element, followed by hydrogen (1.5–8%) and other elements, including oxygen, nitrogen, and sulfur, and small amounts of metals (iron, silicon, calcium, aluminum, sodium, and magnesium). Zinc acetate dehydrate ($Zn(OAc)_2 \cdot 2\ H_2O$, 99%) was obtained from Aladdin and active carbon (coconut shell carbon) was obtained from Fujian SENSEN Carbon.

3.2. Carrier Preparation and Catalyst Synthesis

KOH and petcoke were mixed and ground at a mass ratio of 3:1, mixed thoroughly, and calcined in a tube furnace at a rate of 5 °C/min to 400 °C for 2 h and then 5 °C/min to 850 °C for 2 h, during which N_2 was introduced at a rate of 10 mL/min. This step was followed by washing with 1 mol/L hydrochloric acid and the addition of deionized water to neutralize the mixture to obtain expanded petcoke. A total of 4 g PC was placed in 100 mL wastewater from the plant for 24 h adsorption, followed by drying in a blast drying oven at 80 °C. The dried solid was calcined in a nitrogen furnace at 650 °C for 2 h at a heating rate of 5 °C/min to obtain the desired carrier, which was named PCW. Figure 7 shows a schematic diagram of the preparation.

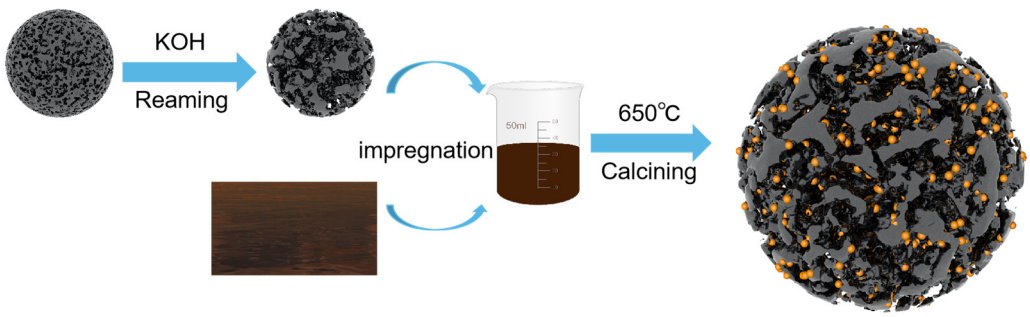

Figure 7. PCW preparation flow chart.

The catalyst used in this study was prepared by the impregnation method. Using the above-prepared PCW as a catalyst carrier, the carrier and zinc acetate were combined at a mass ratio of 1:1 and stirred at 800 r/min for 24 h. Then, the catalyst was dried in a blast drying oven at 80 °C for 12 h. The solid obtained after drying was named Zn/PCW. Under the same conditions, Zn/AC and Zn/PC were prepared using AC (the carrier currently used in industry) and PC as carriers. Zn/PCW(PC) was then calcined in a tube furnace at 500 °C, 600 °C, 800 °C, 900 °C, and 1000 °C for 2 h. The catalysts were calcined at different temperatures to obtain the calcined catalyst, named Zn/PCW-T (where T is the calcination temperature).

3.3. Characterization of Catalysts

ASAP 2460 (Micrometrics Instrument Corporation, Norcross, GA, USA) was used to test the specific surface area, pore volume, and pore size of the samples (degased at 150 °C for 5 h, and then analyzed under liquid nitrogen at −196 °C to test). The specific surface areas, total pore volume, and average pore size were calculated using the Brunauer−Emmett−Teller (BET) and Barrett−Joyner−Halenda (BJH) methods.

The chemical states of elements were analyzed by XPS (Symer Fisher Science, ESCAlAB250Xi, Walthall, MA, USA) using a monochromatic Al Kα X-ray as the excitation source to determine the surface chemical elements of the samples and the C 1 s level of carbon at 284.8 eV was adopted to calibrate the binding energies.

Zinc content was determined by inductively coupled plasma-atomic emission spectroscopy (ICP). A sequential ICP spectrometer Baird ICP 2070 (BEDFORD) with a Czerny Turner monochromator (1 m optical path) was employed.

FTIR (Thermo Scientific, Nicolet IS10, Waltham, MA, USA) was used to identify chemical species (at a resolution of 1 cm^{-1} and accumulating 64 scans using the KBr technique).

The TPD (Micromeritics, ASAP 2720, Norcross, GA, USA) experiment was used to investigate the adsorption and desorption capacity of catalysts for acetylene and acetic acid. All of the tests were conducted with high-purity helium as the purge gas with a flow rate of 115 mL min^{-1}, over the temperature increasing from 50 °C to 800 °C, and a heating rate of 10 °C min^{-1}.

3.4. Catalyst Activity Test

A self-assembled fixed-bed reactor was used for activity testing, as shown in Figure 8. Stainless steel tubes with an inner diameter of 10 mm were loaded with quartz sand and quartz cotton at the bottom for matting, and 2.4 mL catalyst was added. After purification, the pipes were filled with nitrogen. The acetic acid changed from a liquid to a gas at 150 °C and was fed into the heating unit via a peristaltic pump that can control the flow of the liquid. When the temperature reached the reaction temperature of 220 °C, the catalyst was activated with acetic acid for 30 min. The preheater temperature and the reaction temperature were controlled by a CKW-1100 thermal regulator (Beijing Chaoyang Automatic Instrument Factory). Then, the nitrogen valve was closed, the acetylene valve was opened, and the mass flow meter was used to control the flow rate of acetylene to 20 mL/min, so that the acetylene gas and acetic acid vapor mixture and the acetylene and acetic acid were fed with a molar ratio of 3:1. After 30 min of reaction, the waste solution was emptied and the sample tube was used every hour thereafter to pick up the sample. The products were analyzed by a GC-9A gas chromatograph with a PEG/20000 (Zhonghuida, Dalian, China) packed column.

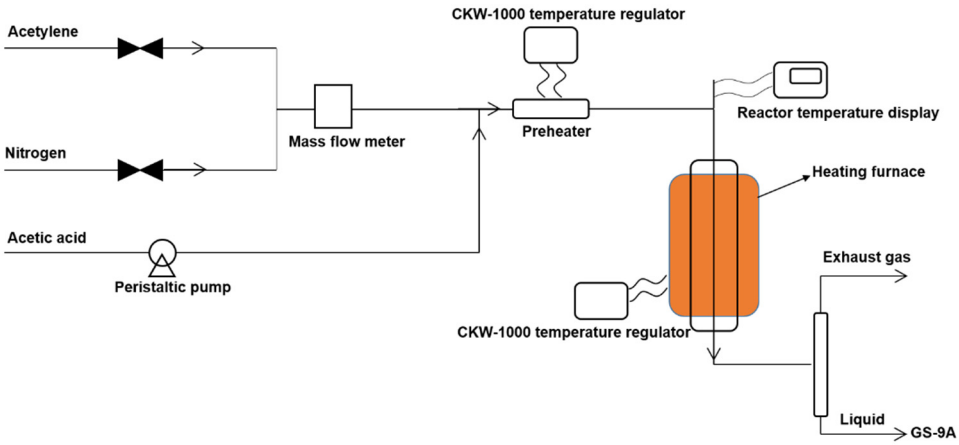

Figure 8. Flow chart of activity determination.

4. Conclusions

In this study, we successfully prepared a novel carrier using petcoke, a by-product of the petroleum industry, and PDW. The Zn/PCW catalyst prepared using this carrier was used for an acetylene acetylation reaction and achieved high activity, which further improved after calcination. Petcoke has many micropores and a large specific surface area, and these characteristics remained after the adsorption of wastewater, which allowed the active component to enter the pore interior to provide more active sites. We screened the calcination temperature and found that its catalytic activity was highest at the calcination temperature of 900 °C, which could reach 85%, and the specific area agent of the catalyst increased with the increase in the calcination temperature, thus making it easier for the raw gas to contact with Zn and the catalytic activity was higher. However, when the temperature exceeded 1000 °C, the content of Zn in the catalyst decreased sharply, resulting in a very low catalytic activity. The introduction of N in the printing and dyeing wastewater reduced the electron cloud density around Zn, making it easier to transfer electrons from acetic acid to Zn. Based on the TPD results, it is also evident that the adsorption of acetic acid by the catalyst is significantly enhanced and, on the contrary, the adsorption of acetylene is reduced. The Zn/PCW catalyst offers significant economic advantages over conventional industrial Zn/AC catalysts and provides a new and valuable treatment for petcoke and PDW.

Author Contributions: X.W. and B.D. designed and conceived the experiments. Y.C. and M.L. performed the experiments. Y.C., Z.X. and G.S. analyzed the data. X.W. and B.D. contributed reagents/materials/analysis tools. Y.C. wrote the paper with direction from X.W. and B.D. All authors have read and agreed to the published version of the manuscript.

Funding: This work was financially supported by the National Natural Science Foundation of China (22178225).

Conflicts of Interest: There are no conflicts to declare.

References

1. Manasrah, A.D.; Nassar, N.N.; Ortega, L.C. Conversion of petroleum coke into valuable products using oxy-cracking technique. *Fuel* **2018**, *215*, 865–878. [CrossRef]
2. Chen, C.; Diao, Y.; Lu, Y.; Chen, S.; Tian, L. Complete Reaction Mechanisms of Mercury Binding on Petroleum Coke and Brominated Petroleum Coke. *Energy Fuels* **2019**, *3*, 5488–5497. [CrossRef]
3. Cao, S.; Chen, Z.; Ma, W.; Zhang, H. Vacuum-assisted and alkali roasting for desulfurization of petroleum coke. *J. Clean. Prod.* **2022**, *332*, 130052. [CrossRef]
4. Hamadeh, H.; Toor, S.Y.; Douglas, P.L.; Sarathy, S.M.; Dibble, R.W.; Croiset, E. Techno-Economic Analysis of Pressurized Oxy-Fuel Combustion of Petroleum Coke. *Energies* **2020**, *13*, 3463. [CrossRef]
5. Ksepko, E.; Klimontko, J.; Kwiecinska, A. Industrial wastewater treatment wastes used as oxygen carriers in energy generation processes. *J. Therm. Anal. Calorim.* **2019**, *138*, 4247–4260. [CrossRef]

6. Shamaei, L.; Khorshidi, B.; Islam, M.A.; Sadrzadeh, M. Industrial waste lignin as an antifouling coating for the treatment of oily wastewater: Creating wealth from waste. *J. Clean. Prod.* **2020**, *256*, 120304. [CrossRef]
7. Wei, G.; Shao, L.; Mo, J.; Li, Z.; Zhang, L. Preparation of a new Fenton-like catalyst from red mud using molasses wastewater as partial acidifying agent. *Environ. Sci. Pollut. Res. Int.* **2017**, *24*, 15067–15077. [CrossRef]
8. Akbarzadeh, R.; Adeniran, J.A.; Lototskyy, M.; Asadi, A. Simultaneous brewery wastewater treatment and hydrogen generation via hydrolysis using Mg waste scraps. *J. Clean. Prod.* **2020**, *276*, 123198. [CrossRef]
9. Choi, J.; Barnard, Z.G.; Zhang, S.; Hill, J.M. Ni catalysts supported on activated carbon from petcoke and their activity for toluene hydrogenation. *Can. J. Chem. Eng.* **2012**, *90*, 631–636. [CrossRef]
10. Zhang, X.; Chen, Z.; Cheng, L.; Xu, L.; Bi, X.; Liu, Q. Valorization of fluid petroleum coke for efficient catalytic destruction of biomass gasification tar. *J. Hazard. Mater.* **2022**, *424*, 127297. [CrossRef]
11. Arcibar-Orozco, J.A.; Zili-Tomita, H.E.; Suárez-Toriello, V.A.; Saucedo-Lucero, J.O. Petcoke Revalorization as Support for ZnO-based Photocatalyst. *Waste Biomass Valorization* **2022**, *13*, 1681–1694. [CrossRef]
12. Mei, S.; Gu, J.; Ma, T.; Li, X.; Hu, Y.; Li, W.; Zhang, J.; Han, Y. N-doped activated carbon from used dyeing wastewater adsorbent as a metal-free catalyst for acetylene hydrochlorination. *Chem. Eng. J.* **2019**, *371*, 118–129. [CrossRef]
13. Wu, X.; He, P.; Wang, X.; Dai, B. Zinc acetate supported on N-doped activated carbon as catalysts for acetylene acetoxylation. *Chem. Eng. J.* **2017**, *309*, 172–177. [CrossRef]
14. Hou, C.; Zhang, X.; Wei., J. A facile synthesis for nitrogen-doped carbon catalyst with high activity of oxygen reduction reaction in acidic media. *Int. J. Energy Res* **2021**, *13*, 45. [CrossRef]
15. Xu, Z.; Zhang, X.; Li, M.; Wang, X.; Zhu, M.; Dai, B. A Highly Active In Situ Zn(CH3COO)2-NC Catalyst for the Acetoxylation of Acetylene. *Ind. Eng. Chem. Res.* **2022**, *61*, 1313–1321. [CrossRef]
16. Liu, X.; Zhai, X.; Sheng, W.; Tu, J.; Zhao, Z.; Shi, Y.; Xu, C.; Ge, G.; Jia, X. Isolated single iron atoms anchored on a N, S-codoped hierarchically ordered porous carbon framework for highly efficient oxygen reduction. *J. Mater. Chem. A* **2021**, *9*, 10110–10119. [CrossRef]
17. Zhang, L.; Wang, J.; Shang, N.; Gao, S.; Gao, Y.; Wang, C. Ultra dispersed cobalt anchored on nitrogen-doping ordered porous carbon as an efficient transfer hydrogenation catalyst. *Appl. Surf. Sci.* **2019**, *491*, 544–552. [CrossRef]
18. Guo, X.; Duan, J.; Li, C.; Zhang, Z.; Wang, W. Modified bamboo-based activated carbon as the catalyst carrier for the gas phase synthesis of vinyl acetate from acetylene and acetic acid. *Int. J. Chem. React. Eng.* **2021**, *19*, 331–340. [CrossRef]
19. Chen, S.; Li, G.; Wang, G.; Yu, B. Structure-activity relationship of zinc acetate/activated carbon catalysts. *J. Catal.* **1986**, *7*, 155–161.
20. Hu, L.; Xu, Z.; He, P.; Wang, X.; Tian, Z.; Yuan, H.; Yu, F.; Dai, B. Zinc and Nitrogen-Doped Carbon In-Situ Wrapped ZnO Nanoparticles as a High-Activity Catalyst for Acetylene Acetoxylation. *Catal. Lett.* **2020**, *150*, 1155–1162. [CrossRef]
21. Islam, M.T.; Dominguez, A.; Alvarado-Tenorio, B.; Bernal, R.A.; Montes, M.O.; Noveron, J.C. Sucrose-Mediated Fast Synthesis of Zinc Oxide Nanoparticles for the Photocatalytic Degradation of Organic Pollutants in Water. *ACS Omega* **2019**, *4*, 6560–6572. [CrossRef]
22. Jeong, S.Y.; Cho, J.S. Porous Hybrid Nanofibers Comprising ZnSe/CoSe(2)/Carbon with Uniformly Distributed Pores as Anodes for High-Performance Sodium-Ion Batteries. *Nanomaterials* **2019**, *9*, 1362. [CrossRef]
23. Li, J.; Kang, L. Non-noble metal single atom catalysts with S, N co-doped defective graphene support: A theoretical study of highly efficient acetylene hydration. *Mater. Today Commun.* **2021**, *27*, 102216. [CrossRef]
24. Zhou, D.; Xie, G.; Hu, X.; Cai, X.; Zhao, Y.; Hu, X.; Jin, Q.; Fu, X.; Tan, X.; Liang, C.; et al. Coupling of kenaf Biochar and Magnetic BiFeO3 onto Cross-linked Chitosan for Enhancing Separation Performance and Cr(VI) Ions Removal Efficiency. *Int. J. Environ. Res. Public Health* **2020**, *17*, 788. [CrossRef]
25. Li, M.; Xu, Z.; Chen, Y.; Shen, G.; Wang, X.; Dai, B. MOFs-Derived Zn-Based Catalysts in Acetylene Acetoxylation. *Nanomaterials* **2021**, *12*, 98. [CrossRef]
26. Jeong, S.Y.; Park, S.-K.; Kang, Y.C.; Cho, J.S. One-dimensional nanostructure comprising MoSe2 nanosheets and carbon with uniformly defined nanovoids as an anode for high-performance sodium-ion batteries. *Chem. Eng. J.* **2018**, *351*, 559–568. [CrossRef]
27. Kent, P.R.C.; Annaberdiyev, A.; Benali, A.; Bennett, M.C.; Landinez Borda, E.J.; Doak, P.; Hao, H.; Jordan, K.D.; Krogel, J.T.; Kylanpaa, I.; et al. QMCPACK: Advances in the development, efficiency, and application of auxiliary field and real-space variational and diffusion quantum Monte Carlo. *J. Chem. Phys.* **2020**, *152*, 174105. [CrossRef]
28. Rong, S.L.; Peng, F.G.; Hong, Z.Z.; Lin, L.Z.; Li, C.M.; Jian, W.; Yuan, F.L.; Feng, L.; Na, L.; Cheng, Z.H. Chiral nanoprobes for targeting and long-term imaging of the Golgi apparatus. *Chem. Sci.* **2017**, *8*, 6829–6835.
29. Javan Bakht Dalir, S.; Djahaniani, H.; Nabati, F.; Hekmati, M. Characterization and the evaluation of antimicrobial activities of silver nanoparticles biosynthesized from Carya illinoinensis leaf extract. *Heliyon* **2020**, *6*, e03624. [CrossRef]
30. He, P.; Wu, X.; Huang, L.; Zhu, M.; Dai, B. Acetoxylation of acetylene to vinyl acetate monomer over bimetallic Zn-Ni/AC catalysts. *Catal. Commun.* **2018**, *112*, 5–9. [CrossRef]